Point-contact and neutron spectroscopy of ruthenium

A. A. Zakharov, S. N. Kraĭnyukov, A. V. Khotkevich, M. B. Tsetlin, Yu. L. Shitikov, M. G. Zemlyanov, M. N. Mikheeva, I. K. Yanson, V. A. Elenskiĭ, and G. P. Kovtun

I. V. Kurchatov Institute of Atomic Energy, Moscow; Physicotechnical Institute of Low Temperatures
(Submitted 27 December 1985)
Zh. Eksp. Teor. Fiz. **91**, 343–351 (July 1986)

The second derivative of the voltage-current characteristic of point contacts and the double differential cross section for inelastic, incoherent neutron scattering have been measured in ruthenium. The experimental results are used to reconstruct the phonon state density $F(\omega)$ and the electron-phonon interaction function $g_{pc}(\omega)$ for various symmetry directions in the single crystal and in a polycrystalline sample. We observe an anisotropy of $g_{pc}(\omega)$ in the single crystal. The functions $g_{pc}(\omega)$ and $F(\omega)$ are consistent in terms of the positions of structural features, differing in the relative heights of these features. The functions $g_{pc}(\omega)$ and $F(\omega)$ are compared with data for other hcp transition metals.

INTRODUCTION

The development of the method of point-contact spectroscopy has opened up some new opportunities for experimentally testing the basic tenets of the elementary theory of metals. Pseudopotential theory makes it possible to calculate the point-contact function of the electron-phonon interaction, $g_{pc}(\omega)$, which differs from the Eliashberg function $g(\omega)$ in having a form factor, which reduces the effectiveness of small-angle processes.[1] For most metals, $g_{pc}(\omega)$ can be determined experimentally in a simple way[2]; for nonsuperconducting metals, point-contact spectroscopy is essentially the only source of information on the spectral function of the electron-phonon interaction. Only for the simple *s-p* metals K, Na, and Cu has the possibility of using microcontact spectra to refine the psuedopotential been demonstrated.[3,4] There is considerable interest in studying the electron-phonon interaction function for transition metals, in order to determine their microscopic characteristics.

Ruthenium is a transition metal with an hcp structure. These metals have attracted interest because the superconducting properties of the various members of this group of metals differ greatly even though they have nearly identical electron state densities at the Fermi level and approximately equal Debye temperatures. For example, the critical temperature of technetium is 7.9 K, and its electron specific heat is $\gamma = 4.3\ \text{mJ/(mole}\cdot\text{K}^2)$ (Ref. 5), while the values for ruthenium are $T_c = 0.5$ K and $\gamma = 3.1\ \text{mJ/(mole}\cdot\text{K}^2)$ (Ref. 6). Neutron studies of the dispersion curves $\omega(\mathbf{k})$ reveal anomalous dips on $\omega(\mathbf{k})$ for $LO[0001]$ phonons near the center of the Brillouin zone[7] in technetium, which has the highest critical temperature T_c among hcp metals. The reason for these dips seems to be a strong selective electron-phonon interaction.[8] It was shown in Ref. 9 that the anomalous temperature dependence of the phonon spectrum and the selective electron-phonon interaction are seen in technetium not only on the differential level but also on the integral level, as a shift of the phonons state density $F(\omega)$ down the energy scale with decreasing temperature and as a difference between the positions of the maxima of $F(\omega)$ and $g_{pc}(\omega)$. It is thus interesting to study and compare $g_{pc}(\omega)$ and $F(\omega)$ in hcp transition metals which have a low critical temperature for the transition to the superconducting state and whose dispersion curves have no anomalies. Ruthenium is a metal of precisely this type; its electron-phonon interaction function $g_{pc}(\omega)$ has not been studied, and there has been little study of the lattice dynamics of Ru. All that we have in the way of experimental data are dispersion curves for phonons in the [0001] direction.[7] The results of model calculations[10–12] of the phonon state density $F(\omega)$ are inconsistent. The Éliashberg electron-phonon interaction function and its transport modifications are not known.

Comparison of the neutron and point-contact spectra of hcp metals is complicated by the significant anisotropy of the functions[2] $g_{pc}(\omega)$, which is seen only weakly for metals with a cubic structure.[13] In a point-contact study of a polycrystalline sample the dimensions of the crystallites are usually much greater than the diameter of the contacts, so that there is always some set of spectra which differ from each other because of different orientations of the crystallites with respect to the axis of the contact. A correct comparison of the phonon state density and $g_{pc}(\omega)$ thus required information on the anisotropy of $g_{pc}(\omega)$. In addition to measuring the point-contact spectrum of the polycrystalline sampled used in the neutron measurements, it is also necessary to carry out a point-contact study of single-crystal samples in various orientations. In addition, a comparison of the point-contact spectra of single-crystal samples with the theoretical functions $g_{pc}(\omega)$ does not require taking an average of the theoretical functions.

In this paper we report an experimental determination of the phonon state density in ruthenium by inelastic incoherent neutron scattering from a polycrystalline sample. We have used the method of point-contact spectroscopy to find the electron-phonon interaction functions $g_{pc}(\omega)$ for the three principal symmetry directions in the single crystal and also in a polycrystalline sample.

EXPERIMENTAL PROCEDURE

The polycrystalline ruthenium is obtained by arc melting in purified argon. It has a resistance ratio $R_{300}/R_{4.2} = 25$

 0038-5646/86/070200-06$04.00

(R_{300} is the resistance of the sample at room temperature, while $R_{4.2}$ is the resistance at liquid-helium temperature). The samples used in the neutron measurements are plates 9 or 4 mm thick, from which prism-shaped samples ≈ 1 cm long are cut for the point-contact spectroscopy. The samples used to study the anisotropy of $g_{pc}(\omega)$ are cut from a single crystal obtained by electron-beam zone melting with a resistance ratio $R_{300}/R_{4.2} = 2500$. Electrochemical polishing of the surfaces of the samples for the point-contact measurements was carried out with an alternating current in a 10% (by volume) aqueous solution of hydrochloric acid. A stainless steel plate served as the second electrode in the polishing.

We studied the characteristics of clamping point-contacts formed by moving two electrodes with respect to each other after they had been brought into contact in liquid helium.[14] The apparatus used to produce the point-contacts not only makes it possible to move the electrodes continuously in the plane in which they make contact with each other but also to adjust the clamping force. In the experiments with single crystals, the orientation of the samples is determined by x-ray diffraction to within 1–2°. The electrodes are mounted in the clamping apparatus in such a way that the axis of a contact runs parallel to the same crystallographic directions in the electrodes. Measurements were carried out for the three principal symmetry directions [0001], [11$\bar{2}$0], and [10$\bar{1}$0]. The precision with which the samples are oriented is determined by the precision which is possible in the visual establishment of two parallel planes (the plane faces of the electrodes, which coincide with the corresponding crystallographic planes and which run perpendicular to the axis of the contact). The deviations were no more than 2–3°.

The point-contact function of the electron-phonon interaction is known to satisfy[1] $g_{pc}(\omega) \propto d^2I/dV^2$, where d^2I/dV^2 is the second derivative of the current-voltage characteristic of the point-contact with respect to $V = \omega/e$, where V is the bias voltage on the contact, and e is the charge of an electron. In the measurements we use a modulation method with a source of a sonic-frequency modulating signal which is operated as either a current source or a voltage source. The dependence of the measured voltage at the second harmonic of the modulating signal on the static voltage on the contact, $V_2(V)$, is proportional to d^2V/dI^2 and d^2I/dV^2, respectively, in these two cases. At a temperature of 1.5 K and for typical levels of the modulating signal, we achieved an energy resolution $\approx$ 1 meV in the spectra. In determining the electron-phonon interaction function $g_{pc}(\omega)$ we converted to d^2V/dI^2 curves into curves of d^2I/dV^2 where necessary and then subtracted the background due to multiphonon processes and the nonequilibrium nature of the phonon subsystem at the contact.[15,16] At present, calculations of $g_{pc}(\omega)$ can be carried out in practice for fewer contacts in the aperture model[1] (the effective diameter of the contact between metal half-spaces separated by a membrane whose thickness is much smaller than the electron mean free path). For the point-contacts which come closest to the aperture model in the purer limit, the absolute intensity of $g_{pc}(\omega)$ is maximized. Consequently, the selection of point-contact spectra with the maximum intensity makes it possible to reconstruct the electron-phonon interaction function which corresponds best to the existing theory.

The point-contact electro-phonon interaction function is found from the expressions

$$g_{Pc}(\omega)+B(\omega) = -\frac{3\hbar v_F}{2^{1/2}e}\frac{\tilde{V}_2(V)}{V_{1,0}^2 d} = -0.699\frac{v_F}{10^6\ \text{m/s}}\frac{\tilde{V}_2(V)}{V_{1,0}^2 d}, \quad (1)$$

$$d = (4/ek_F)(\pi\hbar/R_0)^{1/2} = 45.5\cdot 10^6/k_F R_0^{1/2}. \quad (2)$$

These expressions follow from the basic equations of the theory of point-contact spectroscopy[1] in the approximation of free electrons. Here $V_{1,0}$ is the modulation at $V = 0$, and d is the diameter of the contact in nanometers. The voltages (effective values) are expressed in volts, and the resistance is in ohms. In the case of current regulation we would have $\tilde{V}_2(V) = V_2(V)\,[R_0/R(V)]^3$, where $V_2(V) = V_2(V)\,[R_0/R(V)]^3$ is the second-harmonic voltage taken from the point-contact, $R(V)$ is the differential resistance of the contact, and R_0 is the same, at $V = 0$. In the voltage-regulation case we would have $\tilde{V}_2(V) = V_2(V)\times[1 + R(V)/R_b]$, where $V_2(V) = V_2(V)\times[1 + R(V)/R_6]$ is the second-harmonic voltage taken from the diagonal of the bridge, and $R_b = 10\ \Omega$ is the ballast resistance.

The background function $B(\omega)$ is used in the form proposed in Ref. 13. The background level is characterized by the parameter $\tilde{\gamma} = B/g_{pc}^{max}(\omega)$, where B is the value of $B(\omega)$ at energies above the maximum frequency in the phonon spectrum, and $g_{pc}^{max}(\omega)$ is the maximum value of the point-contact function of the electron-phonon interaction. The value of the Fermi wave vector, $k_F = mv_F/\hbar$, is calculated from the lattice constant of Ru at 4.2 K, $a/c = (2.704\ \text{Å})/4.276\ \text{Å})/(4.276\ \text{Å})$ (Ref. 17) for four electrons per unit cell.

For the neutron measurements we use a time-of-flight spectrometer with a source of cold neutrons.[18] For a coherently scattering system such as the crystal lattice of ruthenium, the experimental method for determining the function $F(\omega)$ is to measure the neutron scattering law in the polycrystalline sample and to average the data over the largest volume in momentum space. The averaging is carried out over the momentum transfer $\varkappa = \mathbf{k}_1 - \mathbf{k}_0$ ($\mathbf{k}_0$,$\mathbf{k}_1$ are the wave vectors of the neutron before and after the inelastic scattering by the lattice site). Here we make use of measurements which were carried out at all scattering angles of the multidetector apparatus of Ref. 18 and also as a result of repeated Bragg scattering of the neutrons in a thick sample. The technique of carrying out the neutron measurements for two different sample thicknesses makes it possible in principle to experimentally test the range of applicability of the incoherent approximation for each of the samples studied and to determine the validity of the reconstructed functions $F(\omega)$.

The test samples are oriented at an angle of 45° with respect to the incident neutron beam in a transmission position. The chopper monochromator is rotated at 11 410 rpm; this monochromator, combined with a beryllium filter, means that the sample is bombarded by a beam of neutrons

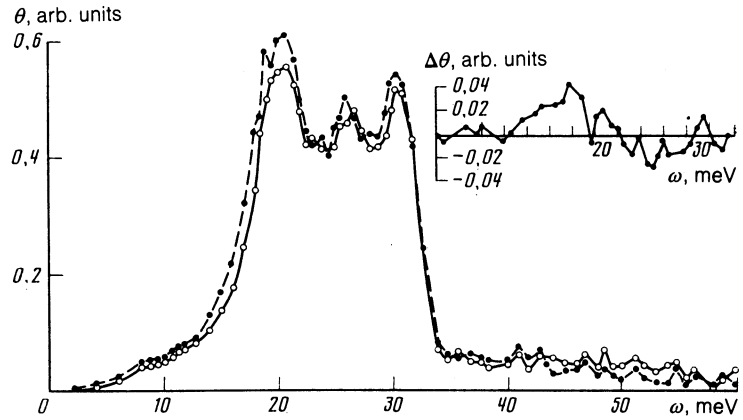

FIG. 1. The energy dependence of the function $\theta(\omega)$ [see (3)] for samples of two thicknesses d: Filled points—$d_1 = 4$ mm; open points—$d_2 = 9$ mm. The inset shows the difference $\theta_1 - \theta_2$, normalized with allowance for multiple scattering.

with a energy of 4.85 ± 0.25 meV, and the energy resolution of the apparatus is better than 7% in the energy-transfer interval[19] (15–35 meV). In addition, measurements were carried out with a width $\tau = 4\,\mu$s of the time-of-flight channel over this energy interval, so we were able to determine the positions of the structural features in the spectrum and its boundary within ± 0.2 meV.

EXPERIMENTAL RESULTS

Figure 1 shows the functions

$$\theta(\omega) \propto \left\langle \frac{k_0}{k_1}\,\omega\left[1-\exp\left(-\frac{\omega}{T}\right)\right]\frac{d^2\sigma}{d\omega\, d\Omega}\right\rangle_{\Omega} \qquad (3)$$

reconstructed in the incoherent approximation from the experimental cross sections for inelastic neutron scattering, $d_2\sigma/d\varepsilon d\Omega$, for two test samples differing in thickness. Here Ω is the difference between the energies of the neutron, $E_1 - E_0$, during inelastic phonon scattering, $\langle \ldots \rangle_\Omega$ means an average over the angles at which the scattered neutrons are detected, and T is the main temperature. Figure 1 shows values of the function $\theta(\omega)$ reconstructed from the neutron spectra, averaged over an interval $\Delta\omega = 0.5$ meV. The curves of $\theta(\omega)$ for the samples of the different thicknesses have not been normalized with respect to each other. It can be seen from these curves that the phonon spectrum of ruthenium has three clearly defined peaks, at 21.1, 26.5, and 30.8 meV. The energy boundary of the spectrum, defined as the position of the half-maximum point on the steep high-energy slope, is $\omega_{up} = 33$ meV. The difference between the $\theta(\omega)$ spectra for the samples of the different thicknesses is a consequence of coherent effects, which fade in importance as the thickness increases. At the same time, however, multiple inelastic processes increase in importance, causing an increase in the state density in the experimental spectra at energies $\omega > \omega_{up}$. Calculations have been carried out on double inelastic scattering of neutrons in the approximation of an infinitely thin plate. Comparison of the results of these calculations with the experimental scattering cross sections shows that the double-scattering cross sections give an essentially complete description of the contribution of multiple processes at $\omega > \omega_{up}$ and can thus be used to describe the multiple scattering over the entire energy range studied. The inset in Fig. 1 shows the difference between the $\theta(\omega)$ functions reconstructed for the different thicknesses, normalized with allowance for multiple scattering.

Figure 2 shows some typical point-contact spectra of the electron-phonon interaction in Ru. Shown here are two curves for each direction and two curves for the polycrystalline samples, which demonstrate the reproducibility of the experimental results.

The error in the position of the peak due to the magnitude of the modulation, the nonzero measurement temperature, and the variation from contact to contact is $+0.5$ meV

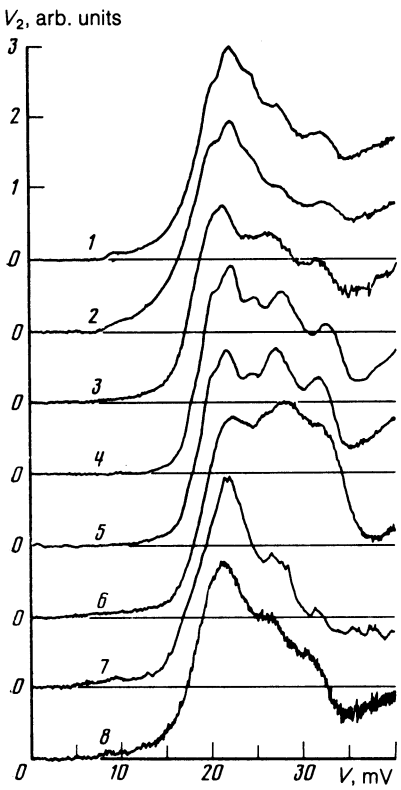

FIG. 2. Point-contact spectra of ruthenium. 1,2—The [0001] direction; 3,4—[11$\bar{2}$0]; 5,6—[10$\bar{1}$0]; 7,8—spectra of a polycrystalline sample. Curve 7 is a plot of $-d^2I/dV^2(V)$, while the other curves are plots of $d^2V/dI^2(V)$. The characteristics of the contacts are listed in Table I. The curve labels correspond to the indices of the contacts given in Table I. The spectra have not been normalized with respect to each other.

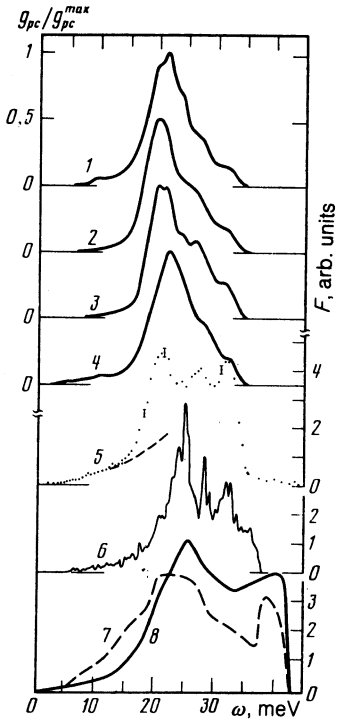

FIG. 3. 1–4—Point-contact electron-phonon interaction functions $g_{pc}(\omega)$ reconstructed from curves 1, 3, 5, and 7 in Fig. 2; 5—phonon state density reconstructed from the function $\theta_2(\omega)$ in Fig. 1; 6, 7, 8—theoretical curves of $F(\omega)$; 6—data from Ref. 12; 7,8—Refs. 10 and 11, respectively.

in this particular case. The point-contact functions reconstructed from curves 1, 3, 5, and 7 in Fig. 2, with the highest intensity, are shown in the upper part of Fig. 3. The contact resistances, the characteristics of the spectra, and the electron-phonon interaction functions are shown in Table I. The point-contact spectra and the electron-phonon interaction functions for the [0001] direction (curve 1 in Fig. 3) have a structural feature at 8–12 meV, which is not found for directions in the basal plane; they have structural features (maxima or knees) at 20, 21.5, 24, 27.5, and 31.5 meV.

For the $[11\bar{2}0]$ direction (curve 2 in Fig. 3), we see a maximum at $\omega = 19$ meV and two peaks at 22 and 31.5 meV. The fine structure in the central part of the spectrum is not seen in high-intensity spectra. In the $[10\bar{1}0]$ direction (curve 3), there are maxima at 20, 21.5, 24, 27.5, and 31 meV.

Curve 4 in Fig. 3 is the electron-phonon interaction function found for a polycrystalline sample. For the spectra of point-contacts between polycrystalline electrodes, the observed variations in the positions and relative intensities of the structural features are small. All the spectra have a main maximum at 21–22 meV, and essentially all have maxima or knees at 27 and 31 meV.

A numerical parameter which characterizes the shape and energy position of the spectrum is the mean square frequency, which is independent of the main value of $g_{pc}(\omega)$:

$$\langle\omega^2\rangle = \int \omega g_{pc}(\omega)\,d\omega \Big/ \int g_{pc}(\omega)\,d\omega/\omega. \qquad (4)$$

Table II shows the minimum, maximum, and mean values of $\langle\omega^2\rangle$ for various directions for all of the spectra which were processed mathematically. We see that the [0001] direction is relatively "soft," while the values of $\langle\omega^2\rangle$ for the polycrystalline samples span a broad interval corresponding to different symmetry directions.

Shown for comparison in Fig. 3 is the phonon state density $F(\omega)$ (curve 5) found as a result of measurement at room temperature. The function $F(\omega)$ was reconstructed from the double differential scattering cross section, with allowance for multiple and many-phonon processes and also the energy dependence of the Debye-Waller factor. The nonzero phonon state density at $\omega > \omega_{up}$ is a consequence of anharmonic effects. At low frequencies, up to 14 meV, the function $F(\omega)$ can be described well by a quadratic law with a Debye temperature $\theta_D = 420$ K (the dashed part of curve 5), in agreement with the value found[20] for θ_D from data on the low-temperature specific heat. The value of $\langle\omega^2\rangle$ for the phonon state density found by replacing $g_{pc}(\omega)$ by $F(\omega)$ in (4) is 517 meV^2.

DISCUSSION OF RESULTS

As can be seen from Figs. 2 and 3, the anisotropy of the electron-phonon interaction in ruthenium is seen as a redistribution of the intensity among the maxima of the point-contact electron-phonon interaction function for the various symmetry directions. The literature reveals previous studies of the anisotropy of the point-contact electron-phonon interaction functions of copper,[13] zinc,[21] tin,[22] and rhenium.[23] In the case of zinc there is a significant anisotropy; the intensity of the spectrum along the hexagonal axis is several times greater than that of the basal plane. The main low-frequency maximum for the hexagonal direction is higher than, and

TABLE I.

Contact	Crystallogr. direction	Measurement temperature, K	R_0, Ω	$V_{1,0}$, μV	V_2^{max} μV	$\bar{\nu}$	$g_{1e}^{max}(\omega)$	λ	$\langle\omega^2\rangle$ MeV^2
1	[0001]	1.50	11.0	466	1.61	0.34	0.80	0.67	463
2	[0001]	1.68	2.5	457	0.74	0.40	0.17	0.17	427
3	$[11\bar{2}0]$	2.85	13.7	416	1.32	0.34	0.94	0.82	464
4	$[11\bar{2}0]$	1.50	0.86	246	0.39	0.26	0.20	0.17	547
5	$[10\bar{1}0]$	1.65	30.1	576	1.46	0.27	0.85	0.94	502
6	$[10\bar{1}0]$	1.50	3.0	245	0.69	0.23	0.64	0.56	507
7	Polycryst.	1.50	7.5	200	0.26	0.25	0.73	0.65	460
8	Polycryst.	1.50	9.0	520	0.75	0.18	0.33	0.31	469

TABLE II.

	Direction	$\langle\omega^2\rangle_{min}$, MeV^2	$\langle\omega^2\rangle_{max}$, MeV^2	$\langle\overline{\omega^2}\rangle$, MeV^2
Single crystal	[0001]	426	464	449±9
	[11$\bar{2}$0]	423	586	501±26
	[10$\bar{1}$0]	502	539	521±8
Polycryst.		447	545	503±12

positioned to the left of, those for the directions in the basal plane. In our case the intensities of the spectra for all directions are approximately the same, and the difference between the hexagonal direction and directions in the basal plane is poorly defined. This difference is characterized by an additional structural feature at 8–12 meV and by fine structure in the main low-frequency maximum. Coherent effects are apparently responsible for the appearance of the same structural features in the neutron spectrum of the thinner sample ($d = 4$ mm; see Fig. 1 and the inset there). The apparent reason for the difference in the anisotropies of the point-contact spectra of Zn and Ru is a difference in the degree of anisotropy of the crystal lattice: For zinc we have $c/a = 1.856$, while for ruthenium we have $c/a - 1.584$, not far from the value of 1.63 corresponding to an ideal hcp lattice.

The point-contact spectrum of a polycrystalline sample (curve 4 in Fig. 3) has three structural features, at positions which are the same, to within experimental error, as those of the corresponding features in the phonon state density (curve 5 in Fig. 3). Also shown in Fig. 3 are theoretical functions $F(\omega)$ found from phenomenological models.[10–12] The most satisfactory agreement is found for the data of Ref. 12, where two coordination spheres were considered in the calculation of the interatomic interaction, and the determination of the force constants used the experimental values of all the elastic moduli c_{ij} and two values of the boundary frequencies of *LO* and *TO* phonons for the [0001] direction, found from data on inelastic coherent neutron scattering. Even in this case, however, the calculated frequencies are too high for longitudinal optical vibrations at certain values of the wave vector. The effect is seen on the theoretical function $F(\omega)$ as an additional structural feature at frequencies above the boundary frequency of the experimental phonon state density.

In comparing the neutron and point-contact spectra, we should call attention to the decrease in the relative intensity of the high-frequency peaks in the point-contact spectra from the value in the neutron spectra. This situation was found for essentially all the transition metals studied.[2] It may be a consequence of the particular selection of phonons in $g_{pc}(\omega)$ in terms of polarization vector[24] in the method of point-contact spectroscopy.

As we have already mentioned, in the ballistic mode of point-contact spectroscopy it is possible to reconstruct the function $g_{pc}(\omega)$ and to use it to determine several important characteristics. One of the most important characteristics of the electron-phonon interaction is the electron-phonon interaction constant

$$\lambda_{pc}=2\int_0^{\omega_{max}} g_{pc}(\omega)\,d\omega/\omega.$$

The maximum absolute intensity of the function $g_{pc}(\omega)$ for Ru is approximately the same as that for Os (Ref. 25): (g_{cp}^{max}(Os) = 0.7). The value of the electron-phonon interaction parameter λ_{pc} averaged over six spectra with the highest intensities is 0.76 ± 0.05. This value of λ_{pc} is high in comparison with that recommended in Grimvall's monograph[26]: $\lambda = 0.4 \pm 0.1$. The value found for λ_{pc}, like the maximum absolute values of the point-contact functions of the electron-phonon interaction, may be no more than an estimate because of our use of the free-electron model in normalizing $g_{pc}(\omega)$ for ruthenium.

Comparing the point-contact electron-phonon interaction functions found for polycrystalline samples of various hcp transition metals with each other and with the corresponding functions $F(\omega)$ (Fig. 4), we note an interesting fact: The point-contact spectra of Ru, Re, and Os are approximately the same in shape and also in terms of the position of the main low-frequency maximum, and the point-contact spectra of Re (Ref. 27) and Ru agree well with the corresponding functions $F(\omega)$ in terms of the positions of the peaks (so far, we have no data on the lattice dynamics of Os). On the other hand, the low-frequency peak in the point-contact spectrum of technetium lies to the left of both the low-frequency point-contact peaks of Re, Ru, and Os (on

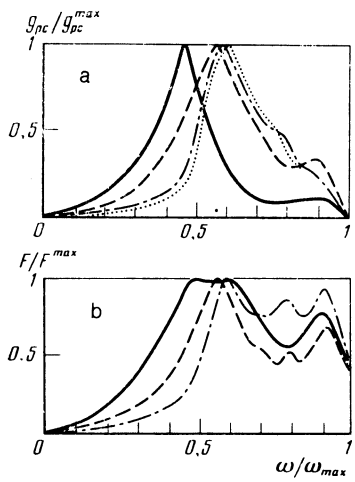

FIG. 4. a: Point-contact electron-phonon interaction functions. b: Phonon state density, in reduced coordinates. Solid lines—Tc (Ref. 9); dashed lines—Re (Ref. 27); dot-dashed lines—Ru (present study); dotted line—Os (Ref. 25).

the one hand) and the feature in its own phonon spectrum (on the other). This result confirms our conclusion regarding the special behavior of the electron-phonon interaction in Tc in comparison with the other hcp transition metals.

Let us summarize the results.

1) The anisotropy of the electron-phonon interaction functions of Ru is manifested as a redistribution of the intensity among the maxima of the point-contact electron-phonon interaction function for various symmetry directions. For the [0001] direction we find an additional structural feature at 10 meV; it is characterized by spectra which are slightly "softer" than for the two other directions. The maximum intensities of the point-contact spectra for the different directions are approximately the same.

2) The functions $g_{pc}(\omega)$ and $F(\omega)$ which we have found agree well with each other in terms of the positions of the structural features, while they differ in the relative intensities of these features. This behavior can be explained in terms of different contributions of phonons with different polarization directions to the point-contact electron-phonon interaction function.

3) Comparison of the point-contact electron-phonon interaction functions and $F(\omega)$ for the various hcp transition metals shows that technetium occupies a special position in this group of metals.

We wish to thank V. P. Polyakovaya for assistance in preparing the polycrystalline ruthenium samples, and we thank A. P. Zhernov and L. A. Maksimov for a discussion of the results of this study.

[1]I. O. Kulik, A. N. Omel'yanchuk, and R. I. Shekhter, Fiz. Nizk. Temp. **3**, 1543 (1977) [Sov. J. Low Temp. Phys. **3**, 740 (1977)].
[2]I. K. Yanson, Fiz. Nizk. Temp. **9**, 676 (1983) [Sov. J. Low Temp. Phys. **9**, 343 (1983)].
[3]A. P. Zhernov, Yu. G. Naĭdyuk, I. K. Yanson, and T. N. Kulagina, Fiz. Nizk. Temp. **8**, 713 (1982) [Sov. J. Low Temp. Phys. **8**, 355 (1982)].
[4]A. P. Zhernov, V. D. Kulagin, and T. N. Kulagina, Fiz. Tverd. Tela (Leningrad) **26**, 587 (1984) [Sov. Phys. Solid State **26**, 354 (1984)].
[5]R. J. Trainor and M. B. Brodsky, Phys. Rev. **B12**, 4867 (1975).
[6]W. Reese and W. L. Johnson, Phys. Rev. **B2**, 2972 (1970).
[7]H. G. Smith and N. Wakabayashi, Solid State Commun. **39**, 371 (1981).
[8]C. Varma and W. Weber, Phys. Rev. Lett. **39**, 1094 (1977).
[9]A. T. Zakharov, M. G. Zemlyanov, M. N. Mikheeva, *et al.*, Zh. Eksp. Teor. Fiz. **88**, 1402 (1985) [Sov. Phys. JETP **61**, 836 (1985)].
[10]R. R. Rao and A. Ramanand, J. Low Temp. Phys. **27**, 837 (1977).
[11]R. R. Rao and A. Ramanand, Phys. Rev. **B19**, 1972, (1978).
[12]R. R. Rao and J. V. S. S. N. Murthy, Z. Naturforsch. **34A**, 724 (1979).
[13]I. K. Yanson, I. O. Kulik, and A. G. Batrak, J. Low Temp. Phys., **42**, 527 (1981).
[14]P. N. Chubov, I. K. Yanson, and A. I. Akimenko, Fiz. Nizk. Temp. **8**, 64 (1982) [Sov. J. Low Temp. Phys. **8**, 32 (1982)].
[15]I. O. Kulik, A. N. Omel'yanchuk, and I. G. Tuluzov, Fiz. Nizk. Temp. **10**, 929, (1984) [Sov. J. Low Temp. Phys. **10**, 484 (1984)].
[16]I. O. Kulik, Pis'ma Zh. Eksp. Teor. Fiz. **41**, 302 (1985) [JETP Lett. **41**, 370 (1985)].
[17]E. O. Hall and J. Grougl, Acta Cryst. **10**, 240 (1957).
[18]M. G. Zemlyanov, A. E. Golovin, and S. P. Mironov, *et al.*, Prib. Tekh. Eksp. No. 5, 34 (1973).
[19]Yu. L. Shitikov, M. G. Zemlyanov, and S. P. Mironov, *et al.*, Prib. Tekh. Eksp. No. 5, 35 (1977).
[20]V. E. Zinov'ev, Kineticheskie svoĭstva metallov privysokikh temperaturakh. Spravochnik (Handbook on the Kinetic Properties of Metals at High Temperatures), Metallurgiya, Moscow, 1984, p. 26.
[21]I. K. Yanson and A. G. Batrak, Zh. Eksp. Teor. Fiz. **76**, 325 (1979) [Sov. Phys. JETP **49**, 166 (1979)].
[22]A. V. Khotkevich and I. K. Yanson, Fiz. Tverd. Tela (Leningrad) **23**, 2064 (1981) [Sov. Phys. Solid State **23**, 1204 (1981)].
[23]N. A. Tulina, Metallofizika **4**, 116 (1982).
[24]A. R. Zhernov, V. D. Kulagin and T. N. Kulagina, J. Phys. **F15**, 579 (1985).
[25]A. V. Khotkevich, V. A. Elenskiĭ, T. P. Kovtun, and I. K. Yanson, Fiz. Nizk. Temp. **10**, 375 (1984) [Sov. J. Low Temp. Phys. **10**, 194 (1984)].
[26]G. Grimvall, The Electron-phonon Interaction in Metals, North-Holland, New York, 1981, p. 256.
[27]M. G. Zemlyanov, N. A. Tulina, and Yu. L. Shitikov, Proceedings of the International Conference of the Physics of Phonons, Budapest, 1985, p. 81.

Translated by Dave Parsons